



Published in final edited form as:

J Clin Neurophysiol. 2016 June ; 33(3): 227–234. doi:10.1097/WNP.0000000000000278.

Automation of Classical QEEG Trending Methods for Early Detection of Delayed Cerebral Ischemia: More Work to Do

Ellis Wickerling¹, Nicolas Gaspard^{2,3}, Sahar Zafar⁴, Valdery Junior Moura⁴, Siddharth Biswal, Sophia Bechek⁴, Kathryn O'Connor⁴, Eric S. Rosenthal⁴, and M. Brandon Westover⁴

¹Department of Technical Medicine, University of Twente, PO Box 217, 7500 AE Enschede, The Netherlands ²Department of Neurology and Comprehensive Epilepsy Center, Université Libre de Bruxelles – Hôpital Erasme, Brussels, Belgium ³Department of Neurology and Comprehensive Epilepsy Center, Yale University School of Medicine, New Haven, CT ⁴Department of Neurology, Massachusetts General Hospital, Boston, MA

Abstract

Objective—The purpose of this study is to evaluate automated implementations of cEEG-based detection of DCI based on methods used in classical retrospective studies.

Methods—We studied 95 patients with either Fisher 3 or Hunt Hess 4-5 aneurysmal SAH who were admitted to the Neurosciences-ICU and underwent continuous EEG monitoring. We implemented several variations of two classical algorithms for automated detection DCI, based on decreases in ADR and RAV.

Results—Of 95 patients, 43 (45%) developed DCI. Our automated implementation of the classical ADR-based trending method resulted in a sensitivity and specificity (Se,Sp) of (80,27)%, compared with the values of (100,76)% reported in the classic study using similar methods in a non-automated fashion. Our automated implementation of the classical RAV-based trending method yielded (Se,Sp) values of (65,43)%, compared with (100,46)% reported in the classic study using non-automated analysis.

Conclusion—Our findings suggest improved methods to detect decreases in ADR and RAV are needed before an automated EEG-based early DCI detection system is ready for clinical use.

INTRODUCTION

Aneurysmal subarachnoid hemorrhage (SAH) accounts for approximately 5% of all strokes. Survivors are at risk for secondary neurologic deterioration due to ischemia and infarction during the subsequent two weeks. This phenomenon, known as delayed cerebral ischemia (DCI), is the major source of long-term neurological disability in survivors of SAH (Haley, Kassell, & Torner, 1992).

Up to 46% of SAH patients may develop DCI (Charpentier et al., 1999), (Hijdra, van Gijn, Nagelkerke, Vermeulen, & van Crevel, 1988), (Hop, Rinkel, Algra, & van Gijn, 1999), (Frontera et al., 1963), (J Claassen et al., 2001). In approximately 25% cases, DCI is clinically ‘silent’ (Jan Claassen, Stephan A Mayer, Kurt T Kreiter, Joseph E Bates, Noeleen Ostapkovich, Adam S Mednick, 2000). Early detection of DCI may prevent permanent neurologic disability by enabling timely interventions, such as initiation of hypertensive therapy, administration of intra-arterial vasodilator therapy, or cerebral angioplasty (Frontera et al., 1963). Currently transcranial Doppler ultrasound, serial clinical examination, and cerebral angiography are chief methods to detect DCI. However, these methods are insensitive and cannot be used in a continuous manner. Consequently DCI often goes undetected or is detected too late for effective intervention.

Two “classical” small yet influential retrospective studies provided evidence that continuous EEG monitoring (cEEG) might allow early detection of DCI (Vespa, 1997), (Jan Claassen et al., 2004). (For a review of other studies that provide additional evidence, see the article in this journal issue by Gaspard.) Decreases in the alpha-delta ratio (ADR) were found in one study to precede many DCI events. (Jan Claassen et al., 2004) A decrease in relative alpha variability (RAV) in the other study was found preceding DCI events (Vespa, 1997). Because the methods in these studies rely on quantitative EEG (QEEG) measures, they lend themselves to automation for continuous prospective DCI surveillance. Nevertheless, more than 10 years later, DCI surveillance using ADR and RAV trending is not routine practice in most medical centers. How well the methods from these pioneering studies perform in practice when implemented in a fully automated fashion remains unclear.

In this study we implemented automated DCI detection algorithms adapted from the classical methods cited above, from Claassen et al 2004 (Jan Claassen et al., 2004) and Vespa et al 1997 (Vespa, 1997). We tested these algorithms on continuous EEG recordings from 95 patients with SAH. We report on the sensitivity and false alarm rates of both automated algorithms for detection of DCI, and explore potential ways to improve their performance.

METHODS

Patient population

All patients with aneurysmal SAH with a Hunt–Hess grade of 4 or 5 (stupor or coma) or a Fisher score 3 or 4 admitted to the Neurosciences ICU (Neuro-ICU) at Massachusetts General Hospital (MGH), Boston between February 2012 and December 2014 were included in the study. Patients with SAH resulting from trauma (non-aneurysmal SAH) were excluded. For our adaptation of the ADR-trending method of Claassen et al (Jan Claassen et al., 2004), we required patients to have a minimum of 24 hours of EEG monitoring to be included in the analysis. For our adaptation of the the RAV trending method of Vespa et al (Vespa, 1997), we required patients to have a minimum of 12 hours of EEG monitoring data to be included in the analysis. Following MGH clinical protocol, EEG monitoring generally started 2 days after the initial SAH and continued for 10 consecutive days, though monitoring times did vary (see manuscript in this issue by Muniz et al for full details). All

data analysis for this study was retrospective and was performed under a protocol approved by the MGH Institutional Review Board.

Definition of DCI

In the literature on aneurysmal SAH, DCI is sometimes divided into two separate categories: radiologically-confirmed delayed cerebral infarction; and delayed ischemic neurologic deterioration, or DIND. Patients were diagnosed with delayed cerebral infarction when a radiologic sign of infarction was present on CT or MRI neuroimaging that was not present on hospital admission and was not attributable to a neurosurgical procedure. DIND was diagnosed in patients who developed a new neurological deficit or significant decrease in Glasgow Coma that was not attributable to a non-ischemic cause. In this study DIND and delayed cerebral infarction were combined into single event, hereafter referred to simply as DCI. For all diagnoses of DCI for this study were determined by a process of independent review of the medical record and subsequent adjudication of any cases of initial disagreements by three study neurologists who were blinded to the EEG findings (MBW, ESR, SZ).

EEG analysis

EEG data was acquired using the standard international 10-20 system. Data was first cleaned using clinical commercially available artefact reduction technology provided as part of the Persyst software suite (Persyst Development Corporation, San Diego, CA). This software uses blind source separation techniques to reduce non-cerebral artefacts in scalp EEG data, and is used routinely in clinical practice at MGH.

ADR and RAV trending were based on EEG data grouped into six regions: Right frontal (F4-C4), left frontal (F3-C3), right rolandic (C4-T4), left rolandic (C3-T3), right posterior (P4-O2) and left posterior (P3-O1). These areas were chosen to roughly correspond to territories of the anterior cerebral artery (ACA), middle cerebral artery (MCA), and posterior cerebral artery (PCA), respectively. (Rubin, Strayer, & Rubin, 2008)

Algorithm for ADR-based DCI Detection

We adapted the method of Claassen et al (Jan Claassen et al., 2004) to create an automated method for detecting DCI based on detection of a decrease in ADR. We note at the outset that this method is not an exact copy of Claassen et al's method, but rather an adaptation using similar principles. See the Discussion section for a more detailed comparison.

For each of the six brain regions described above we computed time-frequency spectrograms using the method of multitaper spectral estimation (Bokil, Andrews, Kulkarni, Mehta, & Mitra, 2010; Bokil, Purpura, Schoffelen, Thomson, & Mitra, 2007; Thomson, 1982), implemented in the Chronux toolbox (<http://chronux.org>). The spectral analysis parameters were: window length $T = 10$ s with no overlap, time-bandwidth product $TW = 3$, number of tapers $K = 5$, and spectral resolution $2W$ of 0.75 Hz.

From each regional spectrogram, for each time t , we calculated the summed power in the 1-4 Hz range, $PA(t)$, and 8-13 Hz range, $PD(t)$. Hereafter we call these frequency ranges the

alpha and delta bands, respectively. Subsequently we calculated the ratio of these sums to form the alpha-delta ratio, ADR:

$$ADR(t) = PA(t) / PD(t) \quad (1)$$

As in Claassen et al (Jan Claassen et al., 2004), we calculated one ADR value each hour. In our adaptation we did this by taking the average ADR value over each hour. Overall, these calculations resulted in 6 ADR time series, each with one ADR measurement per hour for each patient.

Our algorithm attempts to detect DCI by looking for decreases in ADR relative to the baseline value that persist in consecutive measurements some specified number of times. We considered two ways of determining an ADR baseline value:

1. fixed baseline: the first 24 hours of the ADR time series.
2. moving baseline: the previous 24 hours of the ADR time series.

In the method of Claassen et al (Jan Claassen et al., 2004), two parameter value settings that were found to be most promising in terms of sensitivity (Se), specificity (Sp), positive predictive value (PPV), and negative predictive value (NPV) were (1) a decrease in ADR of >10% at least 6 times in row, or (2) any decrease in ADR of >50%. In the present study, as conditions for issuing DCI alarms, we considered ADR decreases relative to baseline of 10%, 20% or 50% over 2, 4, 6, 8, or 10 consecutive measurements. In case more than 10 consecutive below-threshold measurements occurred, we restarted the count over from zero, as illustrated in Figure 1.

Algorithm for RAV-based DCI Detection

We adapted the method of Vespa et al (Vespa, 1997) to create an automated algorithm for detecting DCI based on detection of a decrease in RAV. As above, we note that this method is not an exact copy of Vespa et al's method, but rather an adaptation using similar principles. See the Discussion section for a more detailed comparison.

The initial step in our adaptation of the algorithm is calculating the RAV is to create time series of "alpha to total power ratio" (ATR) values from the 6 regional spectrograms (computed as described above). For RAV the alpha power was defined as the summed power over the range 6-14 Hz (note the slightly different meaning of "alpha" compared with (Jan Claassen et al., 2004)), and the "total" power was the summed power over the 1-20 Hz range. The ATR was defined as the alpha power divided by the total power, multiplied by 100%:

$$ATR(t) = PA(t) / PT(t) \times 100\% \quad (2)$$

These initial ATR time series have a sampling frequency of 0.1Hz (one value every 10 seconds). We next convert these values into a time series of 0.0083Hz (1 value every 2

minutes) by taking the average ATR value within consecutive non-overlapping windows. Finally, we grouped ATR values in these final time series into 12 hour epochs.

As in Vespa et al (Vespa, 1997), each 12 hour epoch was assigned a “relative alpha variability” (RAV) score, ranging from 1 to 4, to characterize the degree of variability during that epoch. The categories are called “poor” (RAV score =1), “fair” (RAV score = 2), “good” (RAV score = 3), and “excellent” (RAV score = 4).

We assigned sequential RAV scores to each of the 6 brain regions in each patient following the method of Vespa et al (Vespa, 1997), as follows (see Table 1). The “baseline” value for each epoch was defined as the median ATR value for that epoch. A “poor” RAV score (RAV=1) was given to epochs with no excursions greater than 2% around the baseline. Epochs with excursions between 2-10% around the baseline were given a “fair” RAV score (RAV = 2). Epochs with excursions of 10% at least every 4 hours were categorized as “good” RAV (RAV = 3).

The criteria for assigning a score of “excellent” RAV (RAV = 4) were not fully specified in (Vespa, 1997); therefore we considered two different options. In the first option RAV = 4 was assigned if there was at least 1 excursion around baseline of at least 15% every hour. In the second option, a score of RAV = 4 was assigned if there were at least 12 excursions of at least 15% around the baseline during the entire 12 hour epoch, regardless of when they occurred.

Following (Vespa, 1997), our RAV-based DCI detection algorithm is “positive” whenever there is a decrease of at least one RAV grade in at least two brain regions during the same epoch.

RESULTS

We identified 95 patients within the study period with aneurysmal SAH. The mean (SD) age of this group was 56.5 (14.7) years. 46 of these patients underwent endovascular coiling, and 49 underwent surgical clipping of their aneurysm. The number of patients who developed DCI was 43 (45%). The mean (SD) time to DCI was 7.5 (3.5) days after onset of SAH. The median [IQR] time from onset of SAH to beginning of EEG monitoring was 61 [42, 84] hours. The median [IQR] duration of EEG monitoring data available for analysis was 154 [97, 196] hours.

For the ADR-based DCI detection method, 85 patients had sufficient EEG data to satisfy inclusion criteria. Of these, 41 (48%) developed DCI. The 12 patients who were excluded lacked the minimal requirement of 24 hours of baseline EEG data needed by the algorithm.

For the RAV-based DCI detection method, 90 patients had sufficient EEG data to satisfy inclusion criteria. 43 of these 90 patients (48%) developed DCI. The 5 patients who were excluded lacked the minimal 12 hours of data required by the detection algorithm.

Results for automated ADR-based DCI detection

Figure 1 illustrates how the ADR-based DCI detection algorithm works. In this example, the ADR trend is shown for the left frontal (LF) region of one patient who had a clinically diagnosed DCI on day 9. In this example there is a clear decreasing trend in ADR values over time. Using the fixed baseline (upper panels) results in a progressively increasing frequency of negative differences relative to baseline. In this case, the trend is so persistent repeated alarms would occur with any of the thresholds we consider, i.e. whether we require anywhere between 0 up to 10 consecutive below-baseline ADR measurements to sound a DCI alarm.

By contrast with the fixed baseline, the moving baseline (lower panels) decreases over time. This results in smaller differences between ADR and baseline and fewer consecutive detections. In this case the DCI alarm may or may not sound, depending on the number of consecutive below-baseline ADR values that we set as an alarm threshold. In this example, we can see that the algorithm would successfully sound the alarm before the clinical diagnosis of DCI on day 9 under a range of possible choices for the alarm threshold.

Unfortunately, despite this encouraging example, in general the trade-off between sensitivity and false alarm rate is not favourable, as we will next see from ROC analysis.

Figure 2 shows points on the receiver operating characteristic (ROC) curve for three threshold values (-10% , -20% and -50%) and for different numbers of consecutive below-baseline ADR measurements used as thresholds to sound an alarm (0, 2, 4, 6, 8 or 10 consecutive measurements). These statistics are based on the entire sample of 85 cases. For comparison, a diagonal “chance line” is shown, representing the sensitivity and specificity values obtainable by sounding an alarm whenever a randomly generated number with uniform probability of taking values between values of 0 and 100% crosses a threshold that likewise varies between 0 to 100%. As is evident from the plots, all ROC points are close to chance performance levels for the fixed baseline method. Slightly better but still poor performance is achieved by the moving baseline method, with highest sensitivity and specificity achieved by requiring 10 consecutive below-threshold ADR values.

Table 2 provides numerical values for the sensitivity, specificity, positive predictive value (PPV) and negative predictive value (NPV) achieved by the ADR-based automated DCI detection algorithm using both fixed and moving baselines. In general, the fixed baseline method gives higher sensitivity but lower specificity, whereas the moving baseline method achieves higher specificity but lower sensitivity. However, as was seen in Figure 2, performance is generally poor for both methods. Under all conditions, adding the sensitivity to the specificity produces values close to 100%, reflecting the observation in Figure 2 that ROC points were generally close to the chance-performance line.

The highest sensitivity and specificity combination (respectively 95% and 34%) achieved by the automated method is obtained with a fixed baseline, a threshold of -10% , and an alarm criterion of 2 consecutive below-baseline ADR values (Table 2). Using these criteria on the clinical cases with DCI the mean time between the first ADR change detection and the

clinical DCI was 3.9 days. As indicated by the low specificity value of 34%, this “early detection” is achieved largely by frequent relatively indiscriminate alarming.

Results for automated RAV-based DCI detection

Figure 3 illustrates how the RAV-based DCI detection algorithm operates. ATR values are plotted every 2 minutes for each of the 6 brain regions, and the RAV score assigned to each 12 hour epoch is plotted above the ATR values. An alarm is emitted for each epoch in which there is a decrease in the RAV score in two or more brain regions. In this case six alarms are issued at different times due to subtle decreases in RAV.

Table 3 shows the sensitivity and specificity achieved by the automated RAV-based detection algorithm for each method of assigning RAV scores, based on the entire sample of 90 cases. Both methods show performance near chance levels, i.e. sensitivity + specificity is nearly equal to 100%. This performance is substantially worse than was achieved by the non-automated method of Vespa et al 1997 (Vespa, 1997) in a cohort of 32 patients, in which sensitivity and specificity were reported to be 100% and 46%, respectively.

Using criterion 1 for assigning an RAV score of 4, the sensitivity and specificity were respectively 65% and 43%. Using this method, in cases with DCI the mean time from the automated alarm to the clinical diagnosis of DCI was 4.7 days. This is earlier than in study of Vespa et al 1997 (Vespa, 1997), where alarms occurred an average of 2.9 days before DCI. However, in the case of our automated RAV-based detection algorithm, given the poor sensitivity and specificity, this lead time reflects the tendency for alarms to occur randomly rather than a true ability detecting events early.

Histograms in figure 4 show the difference in number of alarms for patients with and without DCI. Differences in histograms resulting from option 1 and 2 for assigning scores of RAV = 4 are also demonstrated (left and right Figure columns). In most of the 90 cases in the SAH cohort, no alarm went off, regardless of whether the patient was eventually diagnosed with DCI. In many other cases numerous alarms went off, again without any striking difference between cases with vs without DCI. Using option 1 for assigning scores of RAV = 4 generally results in more alarms than using option 2.

DISCUSSION

In this study we tested whether EEG-based methods modelled after those used in the pioneering retrospective studies of Vespa et al (Vespa, 1997) and Claassen et al (Jan Claassen et al., 2004) could allow early detection of DCI when deployed in a fully automated fashion. Our major finding is that straightforward adaptations of both ADR-based and RAV-based DCI detection algorithms perform at near-chance levels. These findings do not throw doubt on the relationship between cerebral ischemia and spectral changes in the EEG, which are well-established. However, these findings do suggest that further work is required before an automated EEG-based early DCI detection system can be ready for clinical use.

The primary strengths of our study were the relatively large number of cases analysed, and the use of a completely automated, and thus human bias-free, methodology. The algorithms

that we developed employed simple rules to detect decreasing trends in the RAV or the ADR over time. We considered several different criteria for issuing a DCI alarm, by varying the free parameters of each algorithm to optimize statistical measures of performance. The present study was based on relatively large samples of unelected cases (90 cases for RAV-based DCI detection, and 85 cases for ADR-based detection), and performed detections in a completely automated, and thus objective and reproducible way. Our findings are therefore likely to generalize to other groups of patients.

While the automated methods investigated herein were based on methods used in classical retrospective studies, there were important differences in both the findings and in the details of the methodology.

In the study of Claassen et al (Jan Claassen et al., 2004) based on non-automated trending of ADR values, two parameter settings were suggested as particularly promising criteria for issuing DCI alarms: (1) Triggering an alarm upon observing six consecutive ADR values 10% or more below baseline gave a detection sensitivity and specificity (Se,Sp) of (100, 76)%, respectively; (2) triggering an alarm for any ADR decrease of >50% yielded (Se,Sp) = (89,84)%. By contrast, in the present study, observing six consecutive measurements ADR values >10% below baseline, using criterion (1) with a fixed baseline yielded (Se,Sp) = (80,27)%, whereas criterion (2) yielded (Se,Sp) = (44,50)%. Using a criterion of one ADR decrease >50% yielded (Se,Sp)=(90,11)% with baseline criteria (1) and (Se,Sp)=(61,43)% with baseline criteria (2). Both results fall close to chance performance on the ROC plot (Figure 2), indicating that the method performs little or no better than guessing. Changing the algorithm to use a moving baseline resulted in no meaningful improvement in detection performance.

In the study of Vespa et al (Vespa, 1997) using non-automated detection of decreases in RAV, a decrease in RAV by one or more grade resulted in a sensitivity of 100% and a specificity of 46%. By contrast, our automated adaptations of this method performed poorly (Table 1). Using the first of two RAV scoring methods yielded (Se,Sp) = (65,43)%, whereas the second method yielded (Se,Sp)=(42,62)%. Performance of both methods falls near chance levels on the ROC curve, where $Se + Sp = 100\%$.

Our implementation of RAV-based DCI detection causes frequent alarms in patients with and without eventual DCI. Thus, although we found that on average cases of DCI had decreases in RAV 4.7 days before clinically diagnosed DCI, this apparently impressive lead time is unfortunately apparently due to indiscriminate alarming.

The stark contrast between the disappointing results for automated DCI detection in the present work and the promising results of the pioneering studies on which the present work was modelled requires careful consideration. Several important differences between these prior studies and the present study might help to explain these differences while holding out hope that continuous automated DCI detection may yet be possible.

First, in the method of Claassen et al (Jan Claassen et al., 2004), ADR values were evaluated exclusively immediately after clinical staff had stimulated the patient, and presumably at times for which sedating drugs were minimized. In contrast, our automated ADR-based

method used all EEG data. This difference might be critical, as patients at their most alert may have higher ADR values, and ADR values from times of maximal alertness may not be comparable to ADR values obtained at other times. If measuring ADR post-stimulation indeed is critical to obtaining reliable DCI predictions, this would mean that fully automated DCI detection is not entirely possible. Rather, reliable prediction would need to incorporate standardized, regularly timed staff interactions to stimulate the patient, and an efficient means of passing along to the DCI surveillance algorithm the timing of stimulations.

A second probable difference is that in both the methods of Claassen et al (Jan Claassen et al., 2004) and Vespa et al (Vespa, 1997) data epochs were selected manually. It is well known that EEG patterns may be modulated by a wide variety of factors, including sedatives, state changes (e.g. sleep vs wake), metabolic factors, seizures, etc. Thus, while not stated explicitly in the methods sections, it is possible that the manual data selection processes in these prior studies somehow took these factors into account and excluded data for which variations in ADR or RAV had explanations other than DCI. By contrast, in the “naïve automation” approaches explored in the present study, these sources of extrinsic variation remained present in the data, and may have led to frequent alarms.

Overall, we believe that the correct inference from the disappointing findings of the present study are that further work is needed to make automated EEG-based early detection of DCI into a clinical reality. Several mitigating considerations leave room to hope that robust automated DCI detection will eventually be possible. First, the physiological principles underlying EEG-based ischemia detection are well established (Vespa, 1997), (Nagata, Tagawa, Hiroi, Shishido, & Uemura, 1989), (Jan Claassen et al., 2004), (Nuwer, 1987), (Tolonen & Sulg, 1981) (see e.g. the paper by Foreman et al. in this journal issue). Second, subsequent studies using prospective but non-automated approaches to DCI detection based on visual analysis of continuous EEG show promising results (reviewed by Gaspard in this issue; see also the paper by Muniz et al in this journal issue). Third, the attempts made at automation in the present study were relatively unsophisticated from the standpoint of statistical signal processing. Thus, while the present study suggests that “naïve automation” of DCI fails, it is possible that improved methods might yet succeed.

Improvements in case selection might also improve chances of success in future attempts at automated DCI detection. First, several of the cases had common non-DCI complications (e.g. re-hemorrhage, parenchymal ICH, or surgical complications; data not shown) that may produce changes in the EEG similar to those caused by DCI. As in other studies these events were not classified as DCI events, and therefore may complicate the training of any discriminative algorithm. Future work could either exclude such cases, or make special provisions so as to ignore periods surrounding non-DCI complications when training and evaluating detection algorithms. Second, the beginning times and total duration of monitoring varied. Future studies might benefit from restricting analysis to only cases that include data beginning soon after the onset of SAH, e.g. within 48 hours, continue until at least day 6-7, and perhaps by excluding patients who underwent procedures with high rates of confounding complications, e.g. surgical clipping. Of course the downside of stricture inclusion criteria will be that any method developed in this way would have a more limited scope.

Finally, along the same lines, it is likely that a DCI detection algorithm that takes into account covariate factors that affect the EEG (e.g. sedative infusion rates, metabolic factors, times of stimulation) will produce more reliable predictions than algorithms like those in the present study which ignore these factors.

Therefore, while automated EEG-based early detection of DCI is not yet ready for clinical use, we believe that non-automated clinical monitoring for ischemia remains a valuable component of caring for patients with aneurysmal SAH, and remain hopeful that automated continuous EEG-based ischemia monitoring will eventually be possible.

References

- Bokil H, Andrews P, Kulkarni JE, Mehta S, Mitra P. Chronux: A Platform for Analyzing Neural Signals. *Journal of Neuroscience Methods*. 2010; 192(1):146–151. <http://doi.org/10.1016/j.jneumeth.2010.06.020>. [PubMed: 20637804]
- Bokil H, Purpura K, Schoffelen J-M, Thomson D, Mitra P. Comparing spectra and coherences for groups of unequal size. *Journal of Neuroscience Methods*. 2007; 159(2):337–345. <http://doi.org/10.1016/j.jneumeth.2006.07.011>. [PubMed: 16945422]
- Charpentier C, Audibert G, Guillemin F, Civit T, Ducrocq X, Bracard S, Laxenaire MC. Multivariate analysis of predictors of cerebral vasospasm occurrence after aneurysmal subarachnoid hemorrhage. *Stroke; a Journal of Cerebral Circulation*. 1999; 30(7):1402–1408. <http://doi.org/10.1161/01.STR.30.7.1402>.
- Claassen J, Bernardini GL, Kreiter K, Bates J, Du YE, Copeland D, Mayer S. a. Effect of cisternal and ventricular blood on risk of delayed cerebral ischemia after subarachnoid hemorrhage: the Fisher scale revisited. *Stroke; a Journal of Cerebral Circulation*. 2001; 32(9):2012–2020. <http://doi.org/10.1161/hs0901.095677>.
- Claassen J, Hirsch LJ, Kreiter KT, Du EY, Sander Connolly E, Emerson RG, Mayer S. a. Quantitative continuous EEG for detecting delayed cerebral ischemia in patients with poor-grade subarachnoid hemorrhage. *Clinical Neurophysiology*. 2004; 115(12):2699–2710. <http://doi.org/10.1016/j.clinph.2004.06.017>. [PubMed: 15546778]
- Frontera, J. a.; Fernandez, A.; Schmidt, JM.; Claassen, J.; Wartenberg, KE.; Badjatia, N.; Mayer, S. a. Defining vasospasm after subarachnoid hemorrhage: What is the most clinically relevant definition? *Stroke*. 1963; 40(6):1963–1968. <http://doi.org/10.1161/STROKEAHA.108.544700>. [PubMed: 19359629]
- Haley EC, Kassell NF, Torner JC. The International Cooperative Study on the Timing of Aneurysm Surgery. The North American experience. *Stroke*. 1992; 23(2):205–214. <http://doi.org/10.1161/01.STR.23.2.205>. [PubMed: 1561649]
- Hijdra A, van Gijn J, Nagelkerke NJ, Vermeulen M, van Crevel H. Prediction of delayed cerebral ischemia, rebleeding, and outcome after aneurysmal subarachnoid hemorrhage. *Stroke; a Journal of Cerebral Circulation*. 1988; 19(10):1250–1256. <http://doi.org/10.1161/01.STR.19.10.1250>.
- Hop JW, Rinkel GJ, Algra a, van Gijn J. Initial loss of consciousness and risk of delayed cerebral ischemia after aneurysmal subarachnoid hemorrhage. *Stroke; a Journal of Cerebral Circulation*. 1999; 30(11):2268–2271.
- Claassen, Jan; Mayer, Stephan A.; Kreiter, Kurt T.; Bates, Joseph E.; Ostapkovich, Noeleen; Mednick, Adam S.; C., ES.; C., JR. “Silent” cerebral infarction due to vasospasm after SAH [abstract]. *Stroke*. 2000
- Nagata K, Tagawa K, Hiroi S, Shishido F, Uemura K. Electroencephalographic correlates of blood flow and oxygen metabolism provided by positron emission tomography in patients with cerebral infarction. *Electroencephalography and Clinical Neurophysiology*. 1989; 72(1):16–30. [PubMed: 2464472]
- Nuwer M. Evaluation of stroke using EEG frequency analysis and topographic mapping. *Neurology*. 1987

- Persyst Development Corporation. Persyst artifact reduction. (n.d.)Retrieved from <http://persyst.com/artifact-reduction>
- Rubin R, Strayer DS, Rubin E. The nervous system - Circulatory Disorders. Rubin's Pathology. 2008:1189.
- Thomson DJ. Spectrum estimation and harmonic analysis. Proceedings of the IEEE. 1982; 70(9): 1055–1096.
- Tolonen, U.; Sulg, I. a. Comparison of Quantitative Eeg Parameters From Four Different, (mean 53). 1981.
- Vespa P. Early detection of vasospasm after acute subarachnoid hemorrhage usin continuous EEG. Elsevier. 1997; 103:607–615.

Author Manuscript

Author Manuscript

Author Manuscript

Author Manuscript

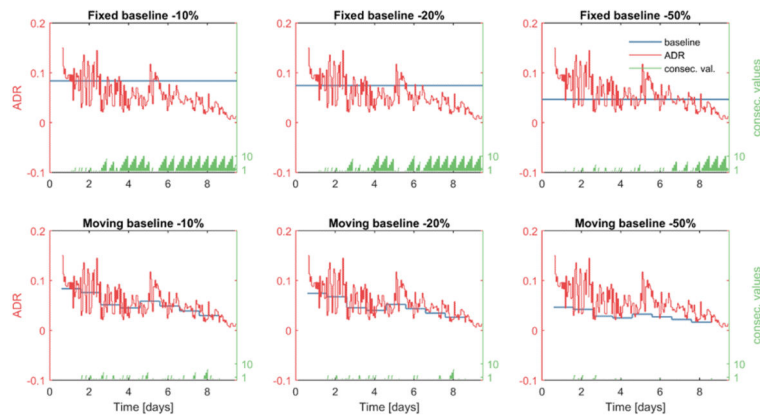


Figure 1.

ADR (red) from the left frontal region of one patient who developed DCI 9 days after SAH. One ADR value is calculated each hour. In the upper plots alarms are determined by comparing ADR values to a constant baseline (blue). In the lower plots alarms are determined by comparing ADR values to a moving baseline (blue). The alarm threshold is set to -10% in the leftmost panels, to -20% in the middle panels, and to -50% in the rightmost panels. The time in days (x axis) represents the time elapsed from the time of initial SAH. The number of consecutive baseline crossings (green) is reset to zero and starts over after exceeding a count of 10.

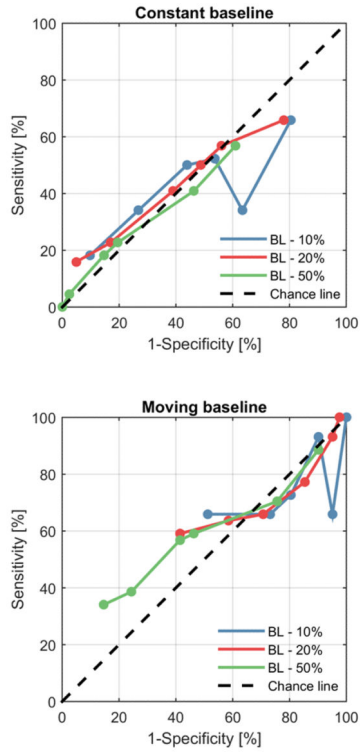


Fig. 2. ROC points for the (A) constant baseline and (B) shifting baseline cases. 1-specificity against sensitivity. Each ROC curve includes 6 points, corresponding to different thresholds (0, 2, 4, 6, 8, 10) on the number of consecutive below-baseline values required to sound an alarm. The different colours represent the three different thresholds. Abbreviations: BL – 10%, alarm threshold is 10% below baseline; BL – 20%, alarm threshold set to 20% below baseline; BL – 50%, alarm threshold set to 50% below baseline.

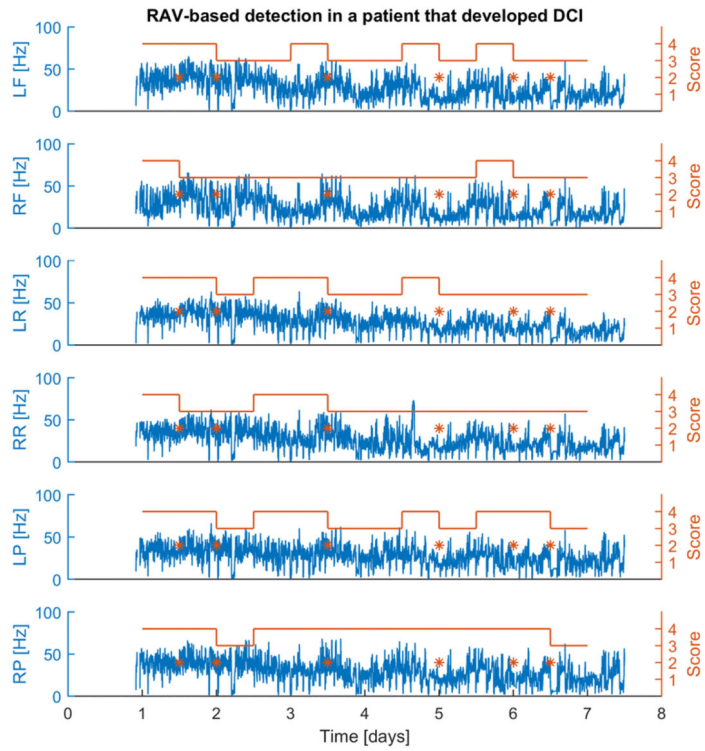


Fig. 3. ATR plots and associated RAV scores for a patient with a clinically diagnosed DCI 7.5 days after onset of SAH. RAV scores are assigned using the scoring rules in Table 1, using option 1 to assign scores of RAV = 4. In this example 6 different alarms are issued during the course of EEG monitoring. The decreases in RAV that lead to the alarms in this case are subtle. Abbreviations: LF/RF, left/right frontal; LR/RR, left/right rolandic; LP/RP, left/right posterior. Time (x-axis) is counted relative to the time of SAH onset.

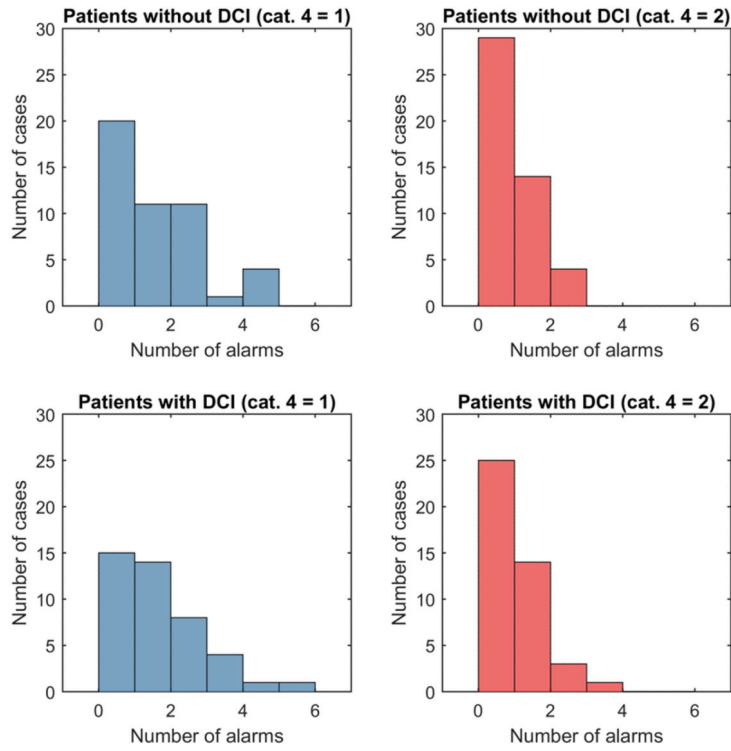


Fig. 4. Histograms of number of alarms vs frequency of alarms. The upper histograms are for patients without clinically diagnosed DCI. The lower histograms are for patients with clinically diagnosed DCI. The left plots result from using option 1 for RAV = 4 and the right plots result from using option 2 (see Table 2).

Table 1

Classification of RAV, adapted from the method of Vespa et al 1997. We considered two methods for assigning a score of 4.

Calculation of RAV scores		
Score:	Description:	Excursions from baseline:
1	Poor RAV	All < 2%
2	Fair RAV	All <10% but some >2%
3	Good RAV	> 10% every 4 hours but not meeting RAV =4 criteria
4	Excellent RAV	Option 1: >15% every hour Option 2: >15% at least 12 times in 12 hours

Author Manuscript

Author Manuscript

Author Manuscript

Author Manuscript

Table 2

Performance statistics for the automated ADR-based DCI detection algorithm, using either a fixed baseline (a) or a moving baseline (b). Thresh, threshold; Sens, sensitivity; Spec, specificity; PPV, positive predictive value; NPV, negative predictive value.

Thresh	successive measurements	Fixed baseline				Moving baseline			
		Sens ^a (%)	Spec ^a (%)	PPV ^a (%)	NPV ^a (%)	Sens ^b (%)	Spec ^b (%)	PPV ^b (%)	NPV ^b (%)
-10%	0	100	0	48	-	80	34	53	65
change	2	95	34	57	88	63	66	63	66
	4	90	7	47	43	54	48	49	53
	6	80	27	51	60	44	50	45	49
	8	73	34	51	58	27	66	42	49
	10	51	34	42	43	10	82	33	49
-20%	0	98	0	48	0	78	34	52	63
change	2	95	7	49	60	56	43	48	51
	4	85	23	51	63	49	50	48	51
	6	71	34	50	56	39	59	47	51
	8	59	36	46	48	17	77	41	50
	10	41	41	40	43	5	84	22	49
-50%	0	90	11	49	56	61	43	50	54
change	2	76	30	50	57	46	59	51	54
	4	46	41	42	45	20	77	44	51
	6	41	43	40	35	15	82	43	37
	8	24	61	37	47	2	95	33	51
	10	15	66	29	45	0	100	-	52

Table 3

Sensitivity (sens.) and specificity (spec.) of the RAV-based automated detection algorithm tested on our cohort of 90 patients, using the two different options for assigning RAV = 4 (see Table 1). For comparison, we also provide here the results reported by Vespa et al 1997 on their cohort of 32 patients.

RAV	Sens.	Spec.
Automated detection (Score 4 – option 1)	65%	43%
Automated detection (Score 4 – option 2)	42%	62%
Vespa et al ⁹	100%	46%

Author Manuscript

Author Manuscript

Author Manuscript

Author Manuscript